Elastic meson form factors with modified vector resonance propagators

Robert A. Williams* and Benjamin Jackson†
Thomas Jefferson National Accelerator Facility, 12000 Jefferson Avenue, Newport News, Virginia 23606
(Received 3 December 1997)

Sakurai's $SU_F(3)$ universality symmetry is employed to provide a unified description of pseudoscalar meson nonet elastic form factors calculated using a modified vector meson dominance (VMD) formalism. We incorporate excited resonances with modified propagators derived from analyticity and elastic unitarity, employing a single channel N/D approximation to model nonresonant meson exchange contributions. Existing spacelike and timelike data for π^+, K^+, and K^0 mesons indicate that finite width corrections to the ρ propagator and couplings are essential for a precise theoretical description in the VMD framework. Our analysis verifies that existing data cannot rule out the possible existence of two unconfirmed resonances (one narrow isoscalar and one broad isovector) just below and above the $p\bar{p}$ threshold previously suggested to explain the anomalous features observed in timelike G_M^p LEAR and G_E^n FENICE data. [S0556-2813(98)04905-X]

PACS number(s): 14.40.Aq, 12.40.Vv, 13.40.Gp

I. INTRODUCTION

Hadronic structure is a topic of fundamental importance in nuclear physics. The distribution of quarks and gluons bound by nonperturbative interactions inside mesons and baryons give rise to a complicated many-body structure which is up to the present time unsolvable from first principles, except for very short distances where perturbative QCD (pQCD) applies. In order to study nonperturbative dynamics of hadronic structure, especially the resonant timelike behavior, we resort to a model calculation based on vector meson dominance (VMD). Although this type of formalism employs effective hadronic interactions with associated phenomenology, a systematic improvement of the theoretical description is possible (in principle) by incorporating rigorous constraints imposed by unitarity, analyticity, and dynamical symmetries. In this work we calculate finite width corrections to the vector meson resonance propagators and include hadronic cutoff effects using a single channel N/D approximation. Elastic unitarity is imposed on individual resonance amplitudes and Cauchy analyticity is enforced, relating the real and imaginary parts of the propagators. In N/D theory, the dynamcial width function of a resonance propagator (related to numerator N of a unitary N/D amplitude) can be consistently calculated from nonresonant exchange amplitudes possessing only left hand cut (LHC) singularities [1,2]. Nonresonant exchange amplitudes are usually neglected in VMD models, however we derive the N functions based on t- and u-channel vector meson exchange amplitudes, thereby modeling effects from nonresonant loop contributions.

Our analysis is motivated in part by results of previously developed models of the nucleon [3] and baryon octet [4] form factors. In Ref. [3] the nucleon form factors were analyzed in a VMD framework and excited vector resonance parameters (i.e., masses, decay widths, and couplings) were adjusted to optimize agreement with the available data. To obtain a good phenomenological description of the timelike LEAR G_M^p [5] and FENICE G_E^n [6] data, two unconfirmed resonance states were included near the $p\bar{p}$ threshold (one narrow $I=0$ state below and one broad $I=1$ state above threshold). Since the timelike meson form factors are fully exposed in this region (i.e., no phase space restrictions) and these ''new'' resonances should also couple strongly to the mesons, we are interested in establishing if resonance signatures from these novel states are present or absent in the existing pion and kaon data. In Ref. [4] the baryon octet form factors were calculated as an extension of the nucleon model by application of Sakurai's universality hypothesis [7], which is an assumed dynamical symmetry relating vector meson couplings to the conserved $SU(3)_F$ hadronic ''charges,'' third component of isospin (I_3), baryon number (B), and strangeness (S). Unfortunately, there is no available data for the strange baryon form factors to test the universality predictions. However, universality symmetry can be applied in the meson sector (reducing the phenomenological freedom) which can then be directly tested against the existing data.

In the next section we discuss our implementation of universality symmetry and its consistency with charge conjugation and G-parity constraints. In Sec. III we discuss our model formalism, deriving modifications to the vector meson propagators from solutions to once subtracted dispersion relations. We present a derivation of the LHC N functions in Sec. IV and discuss our numerical results compared with the available π^+, K^+, and K^0 form factor data in Sec. V. Finally, we summarize our conclusions in Sec. VI. Additional details of the N/D method are presented in the Appendix.

II. $SU_F(3)$ VECTOR MESON UNIVERSALITY

All of the light quark mesons and baryons have electric charges (Q) which are related to the conserved quantum numbers of strong hadronic interactions I_3 (third component of isospin), B (baryon number), and S (strangeness) accord-

*Also at: Department of Physics, Hampton University, Hampton, VA 23668; electronic address: bobw@cebaf.gov
†Also at: Kettering Fairmont High School, Kettering, Ohio, 45429; electronic address: ben2@bigfoot.com

ing to the $SU_F(3)$ flavor symmetry:

$$Q = I_3 + \frac{1}{2}(B+S). \tag{1}$$

Sakurai's universality hypothesis associates each of the conserved quantum numbers of strong interactions with dynamical hadronic charges [7]. This is a natural consequence of boosting $SU_F(3)$ to a local gauge symmetry with the $\rho,\omega,\phi,K^*,\bar{K}^*$ vector mesons interpreted as the gauge bosons of hadronic interactions. Even without this dynamical interpretation, vector meson universality can be viewed as a special limit of $SU_F(3)$ symmetry which may be a good approximation for the vector meson couplings that should be tested empirically.

In our phenomenological implementation of universality symmetry, to each of the three types of vector mesons (ρ,ω,ϕ, including excited states), we associate a coupling to hadrons with strength in proportion to I_3, B, and S. Specifically, the effective ρ,ω,ϕ vector meson couplings to a hadron ($H:|I_3,B,S\rangle$) are expressed as

$$C_\rho(H) = I_3 \cdot C_\rho, \tag{2}$$

$$C_\omega(H) = B \cdot C_\omega^b + S \cdot C_\omega^s, \tag{3}$$

$$C_\phi(H) = B \cdot C_\phi^b + S \cdot C_\phi^s. \tag{4}$$

The effective couplings are defined in VMD as the ratio of hadronic to leptonic decay constants $C_V(H) \equiv g_{VHH}/f_V (V = \rho,\omega,\phi)$. The ω and ϕ each have two types of universal couplings because the physical ω and ϕ eigenstates are orthogonal combinations of the $SU_F(3)$ isoscalar ω_1 (singlet) and ω_8 (octet) states that couple in proportion to baryon number (B) and hypercharge ($Y = B+S$), respectively [8]. Only three of the four isoscalar $C_\omega^{b,s}, C_\phi^{b,s}$ effective couplings are independent since they are related to the $g_{\omega 1}$, $g_{\omega 8}$ hadronic couplings and the SU(3) mixing angle θ (given the experimentally known f_ω, f_ϕ decay constants):

$$C_\omega^b = f_\omega^{-1}(g_{\omega 1}\cos\theta + g_{\omega 8}\sin\theta), \quad C_\omega^s = f_\omega^{-1}(g_{\omega 8}\sin\theta), \tag{5}$$

$$C_\phi^b = f_\phi^{-1}(-g_{\omega 1}\sin\theta + g_{\omega 8}\cos\theta), \quad C_\phi^s = f_\phi^{-1}(g_{\omega 8}\cos\theta). \tag{6}$$

The ϕ is a pure $s\bar{s}$ state and the ω is purely nonstrange when ideal mixing occurs with $\tan\theta = 1/\sqrt{2}$. Note that a nonzero C_ϕ^b violates the empirical Okubo-Zweig-Iizuka (OZI) rule [9], but the possibility of intrinsic nucleon strangeness indicated by several experiments suggest OZI evading ϕNN couplings may exist [10]. If the OZI rule is taken to be exact, then $g_{\omega 8}/g_{\omega 1} = \tan\theta$ (i.e., $C_\phi^b = 0$), and all of the ω couplings to the octet baryons are predicted by Eqs. (3) and (5) with $g_{\omega 8}$ and θ fixed by the kaon data.

An automatic consequence of universality symmetry is that six of the nine meson nonet form factors are determined and consistent with the fundamental constraints from charge conjugation symmetry. Explicitly, we obtain six auxiliary equations:

$$F_\eta = 0, \quad F_{K^-} = -F_{K^+}, \quad F_{\eta'} = 0,$$

$$F_{\bar{K}^0} = -F_{K^0}, \quad F_{\pi^0} = 0, \quad F_{\pi^-} = -F_{\pi^+}. \tag{7}$$

Universality symmetry is also consistent with G-parity conservation since the ω and ϕ states decouple from the pion. We neglect the small G-parity violating ρ-ω mixing effect in this work. Finally, note that the ρ couplings to the kaon are suppressed by 1/2 relative to the pion, hence we recover the usual $SU_F(3)$ prediction.

It is important to realize that the terminology ''universality'' symmetry used in this paper has entirely different meaning compared with the universality (violation) investigated recently by Benayoun *et al.* [11]. These (and other) researchers effectively use the term universality as the approximate equality between the hadronic $g_{\rho\pi\pi}$ and leptonic (f_ρ) decay constants. However, this stronger form of universality is violated by approximately 20% experimentally (if coupling renormalization from finite width propagator corrections are neglected), hence Benayoun *et al.* introduce a fitted parameter (ϵ), interpreted as a measure of universality violation, to account for the observed enhancement in $e^+e^- \to \pi^+\pi^-$ data near the ρ peak. We stress that our usage of the term universality applies only to the symmetry of vector meson coupling strengths relative to different members in $SU_F(3)$ multiplets. Consequently, we have a completely different interpretation for the Benayoun ϵ parameter. Namely, in our model $C_\rho(\pi) = g_{\rho\pi\pi}/f_\rho \approx 1$ by optimization (not constrained by universality), and we reinterpret the Benayoun ϵ parameter as a coupling constant renormalization (δ_ρ in our notation) induced from finite width propagator corrections. In both investigations ρ-coupling enhancement is necessary for a quantitative description of the data [i.e., $C_\rho(\pi) \to C_\rho(\pi)(1+\delta_\rho)$], however, the physical interpretation of the δ_ρ (or ϵ) enhancement depends on the treatment (or neglect) of propagator corrections and the precise definition of universality adopted. In the next section we derive the vector meson propagator corrections and corresponding coupling renormalizations calculated from dispersion relations using LHC vector meson exchange amplitudes derived in Sec. IV.

III. MODEL FORMALISM

The most general current structure of a spin zero meson is expressed as [12]

$$\Gamma_\mu(k,k') = (k'+k)_\mu F(q^2,k^2,k'^2) + (k'-k)_\mu G(q^2,k^2,k'^2), \tag{8}$$

where $k,k',q=(k'-k)$ are the incident meson, final meson, and photon four-momentum, respectively. The coefficients of the two independent Lorentz current structures $(k' \pm k)_\mu$ are the meson form factors F and G. The off-shell form factor G can be related to the F function by application of the Ward-Takahashi identity [13,14]

$$G(q^2,k^2,k'^2) = \left(\frac{k'^2-k^2}{q^2}\right)[F(q^2,k^2,k'^2) - F(0,k^2,k'^2)]. \tag{9}$$

In this paper, we consider only the elastic, on-shell meson form factors where $k^2 = k'^2 = M^2$ and hence the off-shell G

form factors vanish, $G(q^2,k^2,k'^2)\to 0$, and the F form factors depend only on the q^2 virtuality of the photon, $F(q^2,k^2,k'^2)\to F(q^2,M^2,M^2)\equiv F(q^2)$. The off-shell form factor dependence is interesting and relevant to a variety of topics in electronuclear physics [15], however we do not pursue a study of the off-shell dependence in this work.

We now set up dispersion relations relating the real and imaginary parts of the meson form factors and vector meson propagators. In naive VMD, meson form factors are expressed as a simple sum:

$$F_M(s)=\sum_V C_V(M)\frac{\Delta_V^0(0)}{\Delta_V^0(s)}, \tag{10}$$

involving the effective vector meson couplings $C_V(M)$ and the bare resonance propagators

$$\Delta_V^0(s)=M_V^2-s-iM_V\Gamma_V\Theta(s-s_V). \tag{11}$$

The meson charge normalizations imply a sum rule constraint on the vector meson couplings:

$$Q_M=\sum_V C_V(M). \tag{12}$$

Although the charge sum rules may indeed be approximately satisfied, we believe it is unlikely that they should hold exactly due to a suspicious conspiracy between the low-lying and excited vector meson couplings, unless the effective interactions reflect an underlying quark-meson duality. We note that the charge sum rules in naive VMD directly follow from a γ-V transition amplitude which is not gauge invariant for off-shell vector mesons $\mathcal{L}_{\gamma V}=(M_V^2/f_V)\epsilon_\gamma\cdot\epsilon_V$ (i.e., $q\cdot\epsilon_V=0$ only when $q^2=M_V^2$). A more appropriate γ-V transition amplitude is $\mathcal{L}_{\gamma V}=(1/f_V)F_{\mu\nu}^\gamma F_V^{\mu\nu}$, which gives the Feynman rule s/f_V instead of M_V^2/f_V for the γ-V interaction vertex. With this gauge invariant choice, the vector mesons completely decouple from the current at the charge normalization point $s=0$, which makes better sense if we view the meson charges being built up by quark substructure independent of effective hadronic interactions. To be conservative about the physical vector meson couplings and the assumed analytic structure of the meson form factors, we employ VMD to derive resonance dominated spectral functions and then enforce analyticity through a once subtracted dispersion relation:

$$F_M(s)=\mathrm{Re}[F_M(s)]+i\mathrm{Im}[F_M(s)], \tag{13}$$

$$\mathrm{Re}[F_M(s)]=Q_M+\frac{s}{\pi}\mathcal{P}\int\frac{ds'}{s'(s'-s)}\mathrm{Im}[F_M(s')]. \tag{14}$$

In this work we consider finite width corrections to the vector meson propagators induced by nonresonant t- and u-channel vector meson exchange amplitudes. Gounaris and Sakurai were the first to study finite width corrections in VMD using a generalized effective range formulation [16]. Subsequently, Renard showed that the Gounaris and Sakurai model was incompatible with updated experimental data while demonstrating the importance of finite width effects from parametrized LHC contributions using the N/D formalism [17]. In this work, we closely follow Renard's approach. We calculate modified vector meson propagators of the form

$$\Delta_V(s)=M_V^2-s+\Sigma_V(s)-iM_V\Gamma_V(s). \tag{15}$$

Analyticity is implemented through a once subtracted dispersion relation

$$\Sigma_V(s)=M_V^2\left[\delta_V-\left(\frac{s}{M_V^2}\right)\frac{\mathcal{P}}{\pi}\int\frac{ds'}{s'(s'-s)}M_V\Gamma_V(s')\right]. \tag{16}$$

Since the physical vector meson masses should not be shifted at $s=M_V^2$, the subtraction constant δ_V is calculated from the constraint $\Sigma_V(M_V^2)=0$ (for each V state):

$$\delta_V=\frac{\mathcal{P}}{\pi}\int\frac{ds'}{s'(s'-M_V^2)}M_V\Gamma_V(s'). \tag{17}$$

Note that in the narrow width approximation the propagator modifications vanish:

$$\lim_{\Gamma_V\to 0}\delta_V=0, \tag{18}$$

$$\lim_{\Gamma_V\to 0}\Sigma_V(s)=0, \tag{19}$$

$$\lim_{\Gamma_V\to 0}\Delta_V(s)=\lim_{\Gamma_V\to 0}\Delta_V^0(s)=M_V^2-s. \tag{20}$$

The energy-dependent width function is governed by unitarity

$$M_V\Gamma_V(s)=M_V\Gamma_V\frac{\sum_i P_i(s)N_{ii}(s)}{\sum_i P_i(M_V^2)N_{ii}(M_V^2)}, \tag{21}$$

where i sums over hadronic channels coupled to the vector meson (V), $P_i(s)$ are phase space factors ($|\vec{k}|^3/\sqrt{s}$ for a two-body P-wave channel), and $N_{ii}(s)$ are functions (diagonal elements of the ''N matrix'') which possess only left hand cut singularities and incorporate hadronic cutoff effects induced by nonresonant meson exchange. Renard has parametrized the $N_{ii}(s)$ functions and studied inelastic threshold effects in the timelike region, neglecting contributions from exctied resonances [17]. In contrast, we choose to include excited resonances and derive the N functions from vector meson exchange amplitudes, neglecting a model-dependent treatment of inelastic threshold effects. This choice is not arbitrary, rather it follows from a realization that substantial new timelike data has been compiled since Renard's analysis showing resonance structure which appear at energies corresponding to masses of confirmed vector meson excited states. We prefer to look for inelastic threshold signatures by observing features in the timelike data which are not reproduced by the excited resonance states, producing quantitative disagreement with our model. Admittedly, this approach weakens the significance of our extracted resonance couplings, however, treating inelastic channels introduces extra

phenomenology and substantial complications which we do not pursue. We comment further on possible inelastic threshold signatures in the numerical results section.

For each (low lying and excited state) vector meson, the imaginary part of the resonance propagator (dynamical width function) simplifies according to our approximations, taking the form

$$M_V\Gamma_V(s)=M_V\Gamma_V P_V(s)L_V(s), \tag{22}$$

where $P_V(s)$ is the normalized two-body phase space function

$$P_V(s)=\frac{(s-s_V)^{3/2}}{\sqrt{s}}\frac{M_V}{(M_V^2-s_V)^{3/2}}, \tag{23}$$

depending on the threshold mass $s_V=(2M_\pi)^2,(3M_\pi)^2,(2M_K)^2$ for the ρ, ω, and ϕ propagators, respectively. $L_V(s)$ is the normalized hadronic form factor derived from vector meson exchange N_V functions:

$$L_V(s)=\frac{N_V(s)}{N_V(M_V^2)}. \tag{24}$$

We discuss our derivation of the $N_V(s)$ functions in the next section.

Before passing to our derivation of the N_V functions, we collect our results and obtain the meson $M=\pi^+,K^+,K^0$ form factor spectral functions

$$\mathrm{Im}[F_M(s)]=\sum_V \Theta(s-s_V)C_V(M)\left(\frac{\Delta_V(0)}{\Delta_V^0(0)}\right)s\frac{M_V\Gamma_V(s)}{|\Delta_V(s)|^2}. \tag{25}$$

Our model spectral functions reproduce the naive VMD form factors in the limit when the vector resonance widths are taken to zero (narrow width approximation), the excited states are neglected, and the effective couplings are constrained by the charge normalization sum rules. The factor $\Delta_V(0)/\Delta_V^0(0)=1+\delta_V$ gives a finite width enhancement to the effective vector meson couplings and a corresponding enhancement of the resonant cross section. As noted in the work of Renard [17], the timelike pion and kaon form factors show an enhancement relative to naive VMD. In addition to the enhanced (renormalized) vector meson couplings, Renard demonstrated that a dynamical suppression of the decay width function contributes to the observed timelike enhancement. Our model produces timelike enhancement for related but substantially different reasons. We demonstrate the timelike enhancement effects in the numerical results section along with a more detailed discussion.

IV. LHC EXCHANGE AMPLITUDES

The most important finite width corrections apply to the ground state ρ-meson propagator due to its large hadronic couplings to the $\pi\pi$ and KK channels, and its relatively large decay width (compared with the ω and ϕ). However, we attempt to treat all vector mesons on equal footing, realizing that our derived $N_V(s)$ functions for the ω, ϕ, and all excited states suffer from specific ambiguities (discussed below) which do not apply to the ground state ρ meson. Fortunately, our treatment of the narrow ω, ϕ produce negligible propagator corrections, and the broad excited states contribute terms with very small effective couplings, rendering the excited state propagator modifications inconsequential.

As a starting point, we explicitly consider the ground state ρ-meson N_ρ function and then discuss problems and ambiguities associated with the excited and isoscalar states. To derive the LHC N_ρ function, we assume the dominant nonresonant amplitude in elastic $\pi\pi$ scattering comes from t- and u-channel ρ-meson exchange. This approximation is borrowed from the Chew-Mandelstam bootstrap idea where the ρ-resonance can be generated by a potential derived from ρ-exchange amplitudes [18]. In N/D theory, the pole structure and cut discontinuities of the N and D functions are intimately related through crossing symmetry and analyticity. Several authors have studied bootstrap dynamics for the resonant $\pi\pi$ [19–22], $\rho\pi$ [23], and $K\bar{K}$ [24] amplitudes employing the N/D method and crossing symmetry. For a review of bootstrap applications using the N/D method see Ref. [25]. In contrast to our approach (i.e., calculating the LHC N_ρ function from meson exchange), the recent work of Benayoun *et al.* incorporates a VMD unitarization prescription based on a minimal implementation of N/D theory incorporating a best-fit phenomenological LHC parametrization [11].

Consider the covariant tree-level elastic $\pi\pi$ scattering amplitude based on ρ-meson t- and u-channel exchanges:

$$T^\rho_{\pi\pi}(s,t)=g^2_{\rho\pi\pi}\frac{[F^2_{\rho\pi\pi}(t)(u-M_\rho^2)(s-u)+F^2_{\rho\pi\pi}(u)(t-M_\rho^2)(t-s)]}{(t-M_\rho^2)(u-M_\rho^2)}, \tag{26}$$

where $F_{\rho\pi\pi}(x)$ $(x=t,u)$ is a purely real, hadronic $\rho\pi\pi$ vertex form factor with no singularities for spacelike momentum transfer $(t,u<0)$. Since $F_{\rho\pi\pi}(x)$ should satisfy a once subtracted dispersion relation with the same spectral function as the pion form factor, $\mathrm{Im}[F_{\rho\pi\pi}(s)]\propto\mathrm{Im}[F_\pi(s)]$ $(s>4M_\pi^2)$, a reasonable approximation is to take the ρ-meson mass as the appropriate hadronic cutoff scale for spacelike momentum transfer (analogous to naive VMD for F_π). This approximation also reveals an embeded functional dependence between the nonresonant LHC N functions and the resonant RHC D functions $N(D(N(D(\cdots))))$. Adopting the naive VMD form factor

$$F_{\rho\pi\pi}(x)=\frac{M_\rho^2}{M_\rho^2-x}, \tag{27}$$

we obtain the nonresonant, Born $\pi\pi$ scattering amplitude depending only on the Mandelstam variables (s,t,u), the $\rho\pi\pi$ coupling constant $(g_{\rho\pi\pi})$, and the ρ mass (M_ρ),

$$T^{\rho}_{\pi\pi}(s,t)=g^2_{\rho\pi\pi}M^4_\rho\frac{[(u-M^2_\rho)^3(s-u)+(t-M^2_\rho)^3(t-s)]}{(t-M^2_\rho)^3(u-M^2_\rho)^3}. \tag{28}$$

Using the kinematic relations (in the $\pi\pi$ c.m. system):

$$s=4(|\vec{k}|^2+M^2_\pi), \tag{29}$$

$$t=2|\vec{k}|^2(\cos\theta-1), \tag{30}$$

$$u=-2|\vec{k}|^2(\cos\theta+1), \tag{31}$$

and projecting onto the P-wave partial amplitude, we find

$$T^{\rho}_{\pi\pi}(s)|_{l=1}=\frac{g^2_{\rho\pi\pi}}{2}M^4_\rho(-4|\vec{k}|^2)\times\int^1_{-1}dx\frac{[A(s)x^2+B(s)]x^2}{[C(s)(1-x^2)+D(s)]^3}, \tag{32}$$

where

$$A(s)=48|\vec{k}|^6+4|\vec{k}|^4(3M^2_\rho+4M^2_\pi), \tag{33}$$

$$B(s)=80|\vec{k}|^6+12|\vec{k}|^4(7M^2_\rho+4M^2_\pi)+24|\vec{k}|^2M^2_\rho\times(M^2_\rho+2M^2_\pi)+M^4_\rho(M^2_\rho+12M^2_\pi), \tag{34}$$

$$C(s)=4|\vec{k}|^4, \tag{35}$$

$$D(s)=M^2_\rho(4|\vec{k}|^2+M^2_\rho). \tag{36}$$

The integral Eq. (32) can be evaluated in closed form:

$$T^{\rho}_{\pi\pi}(s)|_{l=1}=(4g^2_{\rho\pi\pi}|\vec{k}|^2)M^4_\rho\left[\frac{AC+BC+AD}{4C^2D^2}-\frac{5AC+BC+5AD}{8C^2D(C+D)}-\frac{BC-3A(C+D)}{8C^{5/2}(C+D)^{3/2}}\times\tanh^{-1}\sqrt{\frac{C}{C+D}}\right], \tag{37}$$

$$T^{\rho}_{\pi\pi}(s,s_\rho)|_{l=1}=(4g^2_{\rho\pi\pi}|\vec{k}|^2)M^4_\rho\left[\frac{-32|\vec{k}|^6+4|\vec{k}|^4(M^2_\rho-s_\rho)+6|\vec{k}|^2M^4_\rho+M^6_\rho}{4|\vec{k}|^4M^4_\rho(4|\vec{k}|^2+M^2_\rho)^2}-\frac{1}{8|\vec{k}|^6}\tanh^{-1}\left(\frac{2|\vec{k}|^2}{2|\vec{k}|^2+M^2_\rho}\right)\right]. \tag{38}$$

Equation (38) is explicitly written in terms of the ρ-threshold variable $s_\rho=(2M_\pi)^2$ (the RHC threshold energy) anticipating the generalization to ω and ϕ mesons. To identify the correct definition for $N_\rho(s)$, we write the full P-wave N/D amplitude (including both resonant and nonresonant contributions) for elastic $\pi\pi$ scattering

$$\mathcal{T}^{l=1}_{\pi\pi}(s)=\frac{\mathcal{N}_{\pi\pi}(s)}{\mathcal{D}_{\pi\pi}(s)}, \tag{39}$$

which satisfies the two-body elastic unitarity equation,

$$\mathrm{Im}[\mathcal{T}^{l=1}_{\pi\pi}(s)]=\frac{1}{16\pi}\frac{|\vec{k}(s)|}{\sqrt{s}}|\mathcal{T}^{l=1}_{\pi\pi}(s)|^2\Theta(s-4M^2_\pi), \tag{40}$$

to define the N_ρ-function:

$$\mathcal{N}_{\pi\pi}(s)\equiv\frac{2}{3}(4g^2_{\rho\pi\pi}|\vec{k}(s)|^2)\frac{N_\rho(s)}{N_\rho(M^2_\rho)}, \tag{41}$$

$$\mathcal{D}_{\pi\pi}(s)\equiv\mathrm{Re}[\Delta_V(s)]-iM_\rho\Gamma_\rho(s), \tag{42}$$

$$M_\rho\Gamma_\rho(s)=\frac{2}{3}\frac{g^2_{\rho\pi\pi}}{4\pi}\frac{|\vec{k}(s)|^3}{\sqrt{s}}\frac{N_\rho(s)}{N_\rho(M^2_\rho)}. \tag{43}$$

Finally, we identify the N_ρ function with the LHC amplitude by factoring out the phase space factor appearing in the numerator function of the unitary N/D amplitude (neglecting overall constants which drop out due to the normalization constraint)

$$T^{\rho}_{\pi\pi}(s,s_\rho)|_{l=1}\equiv|\vec{k}(s,s_\rho)|^2N_\rho(s,s_\rho), \tag{44}$$

which gives $N_\rho(s)\equiv N_\rho(s,s_\rho)$ as the expression inside the square brackets of Eq. (38). In Eq. (44) the threshold energy variable s_ρ is written explicitly, and the two-body c.m. momentum function is generalized for $V=\rho,\omega,\phi$ states:

$$|\vec{k}(s,s_V)|=\frac{1}{2}(s-s_V)^{1/2}. \tag{45}$$

Normalizing according to Eq. (24), $L_\rho(s)=N_\rho(s)/N_\rho(M^2_\rho)$, we obtain the LHC form factor of the ρ propagator employed in our numerical calculations. For the excited ρ propagators we originally assumed the same LHC form factor normalized to the excited mass:

$$L_{\rho'}(s)=\frac{N_\rho(s)}{N_\rho(M^2_{\rho'})}. \tag{46}$$

However, with this ansatz the minimum of $\Sigma_{\rho'}(s)$ does not correspond to the ρ' mass, which is necessary so that the modified propagator reduces to the bare propagator when nearly on mass shell [i.e., $\Sigma'_V(M^2_V)=0$]. This constraint on the minimum position would be automatically satisfied with

a twice subtracted propagator dispersion relation, however, using the once subtracted dispersion relation Eq. (16) we are able to produce a consistent (approximate) minimum position for the excited states if the ρ mass is replaced by the excited ρ' mass in the ρ cutoff function

$$N_{\rho'}(s)=N_{\rho}(s|M_{\rho}\to M_{\rho'}). \tag{47}$$

This excited state ansatz generalizes the crossing bootstrap duality noted in the derivation of the ρ-meson cutoff function. We believe that this *bootstrap duality* hypothesis (where the resonance mass sets the scale for the LHC form factor and vice versa) is suspicious and even unlikely for the excited states, however, we stress that our resulting meson form factors are numerically insensitive to the excited state propagator modifications, which are included so that all resonance states are consistently treated using the same approximations.

Next consider the ω and ϕ propagators where certain ambiguities become aparent that do not affect the ρ propagator. For example, the ω is not a $\pi^+\pi^-$ resonance (neglecting ρ-ω mixing) due to G-parity and thus the ω propagator should connect three-pion and/or $\rho\pi$, $K\overline{K}$, ..., two-body states. We assume the LHC N_{ω} function can be described by ω exchange for elastic $\rho\pi$ scattering, extrapolating to the three-pion threshold by the replacement

$$|\vec{k}[s,s_{\omega}=(M_{\rho}+M_{\pi})^2]|\to|\vec{k}[s,s_{\omega}=(3M_{\pi})^2]|. \tag{48}$$

Although the $\omega\rho\pi$ interaction has different Lorentz structure compared with $\rho\pi\pi$, we assume the same functional form for the ω cutoff function $N_{\omega}(s)$ through the ansatz

$$N_{\omega}(s)=N_{\rho}(s,s_{\rho}\to s_{\omega}|M_{\rho}\to M_{\omega}). \tag{49}$$

The excited ω' states are treated using the same bootstrap duality prescription previously discussed for the ρ' states:

$$N_{\omega'}(s)=N_{\omega}(s|M_{\omega}\to M_{\omega'}). \tag{50}$$

For the ϕ-meson propagator, all types of vector meson (ρ,ω,ϕ) exchanges are allowable for the nonresonant $K\overline{K}$ scattering amplitude. Also, the RHC threshold starts at $s_{\phi}=(2M_K)^2>>(2M_{\pi})^2$. In light of the fact that the ϕ meson is extremely narrow and we expect very small propagator corrections, we are not motivated to develop a sophisticated treatment for the ϕ, hence we simply apply the bootstrap duality prescription. Our treatment of all ground and excited state vector mesons can be summarized by the single equation

$$N_V(s)=N_{\rho}(s,s_{\rho}\to s_V|M_{\rho}\to M_V), \tag{51}$$

where $s_V=(2M_{\pi})^2$ for $V=\rho,\rho',\rho'',\rho'''$, $s_V=(3M_{\pi})^2$ for $V=\omega,\omega',\omega'',\omega'''$, and $s_V=(2M_K)^2$ for $V=\phi$ propagators.

V. NUMERICAL RESULTS

Before discussing our form factor results, we first show the numerical effects of the vector meson propagator modifications. In Fig. 1 we show the normalized cutoff functions of the ρ and excited isovector mesons, $L_V(s)=N_V(s)/N_V(M_V^2)$ for $V=\rho,\rho',\rho'',\rho'''$. All isoscalar vector meson cutoff functions have similar shape and produce negligible effects on the meson form factors, hence we do not show them. In Fig. 2 we show the effect of $L_{\rho}(s)$ on the dynamical ρ-width function by comparing the static width, phase space modified width, and full dynamical width (including phase space and LHC form factor). The cutoff form factor gives very mild off-shell suppression, which gives a pragmatic justification for our use of once subtracted dispersion relations. We plot the exact numerical and approximate parametrized solutions of the propagator dispersion relation for $\Sigma_{\rho}(s)$ Eq. (16) in Fig. 3. Our approximate solutions are expressed in terms of a function depending on three parameters (ξ_V,γ_V,β_V):

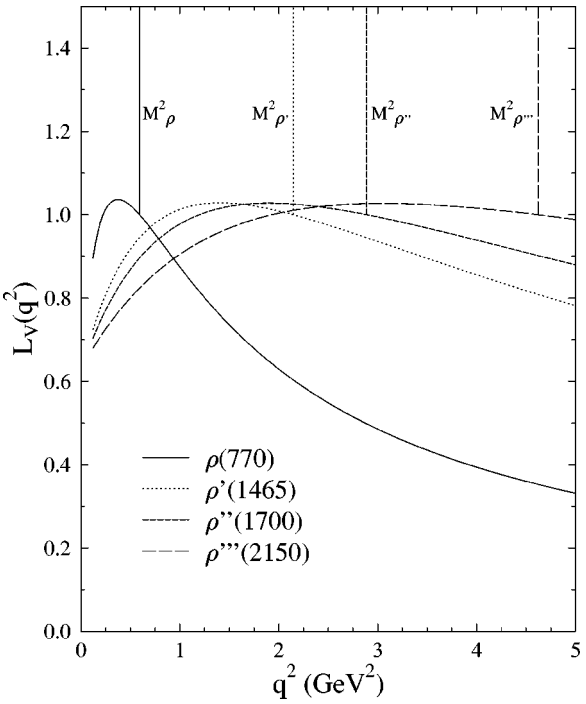

FIG. 1. Normalized LHC form factors of the isovector resonances.

$$\Sigma_V(s)=\frac{\delta_V(|\xi_V|^{\gamma_V}+1)(M_V^2-s)^2}{M_V^2[|\beta_V(s/M_V^2)+\xi_V|^{\gamma_V}+1]}. \tag{52}$$

This form automatically satisfies the constraints $\Sigma_V(M_V^2)=0$ and $\Sigma_V'(M_V^2)=0$. Note that δ_V is a solution to the constraint Eq. (17) (for each V) and thus is not a free parameter of the fit. Physically, δ_V provides a finite width enhancement of the vector meson couplings near $s=M_V^2$. Our result for the ρ enhancement factor $\delta_{\rho}=0.145$ derived from Eq. (17) compares favorably with the experimentally observed enhancement seen in the resonant $e^+e^-\to\pi^+\pi^-$ cross section near the ρ peak, $\delta_{\rho}=0.13\pm0.08$ [26,27]. All vector meson parameters (masses, widths, couplings) are listed in Table I together with our model predictions for δ_V. The exact numerical solutions of the meson form factors using the dispersion relation Eq. (14) with the spectral functions given by Eq. (25) are well approximated by a simple sum of terms analogous to naive VMD:

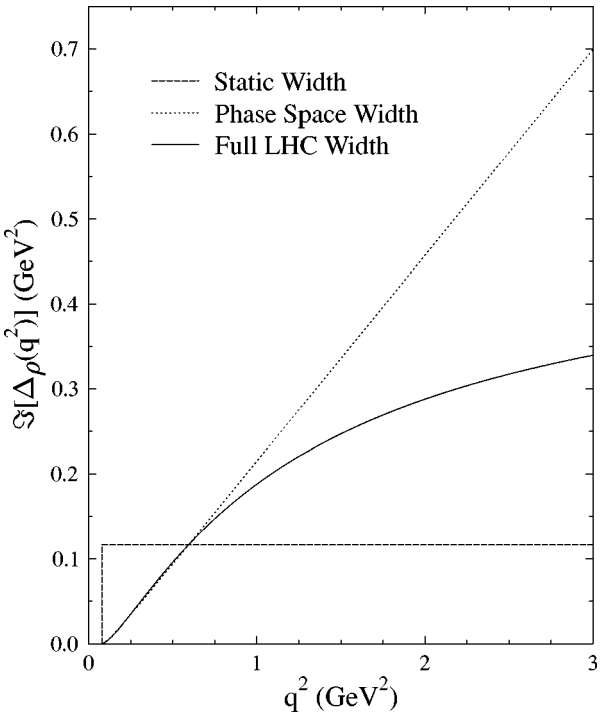

FIG. 2. Imaginary part of the ρ propagator $M_\rho\Gamma_\rho(s)$ comparing three approximations: static width, $M_\rho\Gamma_\rho(s)=M_\rho\Gamma_\rho\Theta(s-4M_\pi^2)$ (dashed line), phase space width, $M_\rho\Gamma_\rho(s)=M_\rho\Gamma_\rho P_\rho(s)\Theta(s-4M_\pi^2)$ (dotted line), and full width, $M_\rho\Gamma_\rho(s)=M_\rho\Gamma_\rho P_\rho(s)L_\rho(s)\Theta(s-4M_\pi^2)$ (solid line).

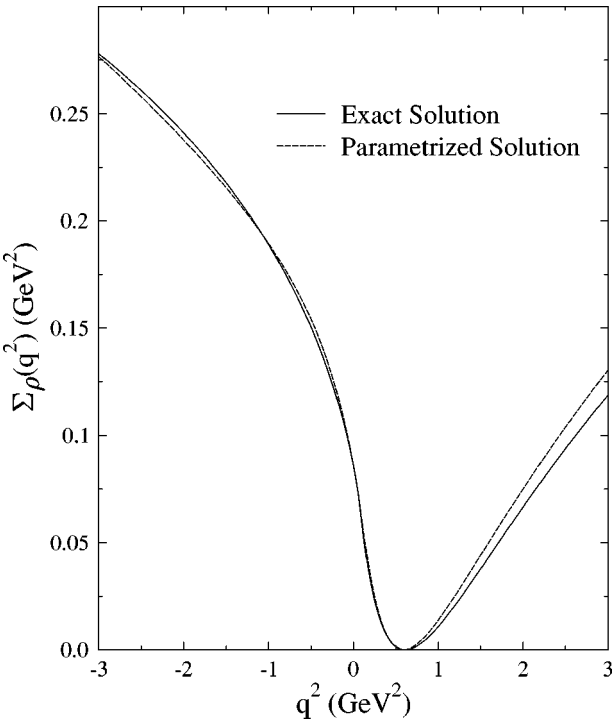

FIG. 3. Finite width correction to the real part of the ρ propagator comparing the exact numerical solution of Eq. (16) (solid line) and the approximate parametrized solution given by Eq. (52) (dashed line).

$$F_M(s)=Q_M+\sum_V C_V(M)(1+\delta_V)\left(\frac{s}{\Delta_V(s)}\right), \qquad (53)$$

expressed in terms of the (calculated) finite width enhancement factors (δ_V) and modified vector meson propagators [$\Delta_V(s)$] using the parametrized solutions of Eq. (52). Besides the modified propagators and coupling constant renormalizations, Eq. (53) differs from naive VMD by the factor of s in the numerator replacing the usual M_V^2. As we previously discussed, this factor of s follows from a gauge invariant treatment of the γ-V interaction, and implies that the vector mesons decouple from real photons, freeing the effective couplings from charge sum rule constraints. We now discuss our form factor numerical results showing observable effects following from our modifications to naive VMD.

We include all of the well-established vector mesons with mass below 2.0 GeV [except the $\phi^*(1680)$], fixing their masses and decay widths to the experimentally measured values quoted in the Particle Data Group's review of particle properties [28]. We also investigate possible effects from two unestablished excited states, the $\omega'''(1830)$ and $\rho'''(2150)$, which were shown to be crucial for a quantitative description of the precise LEAR G_M^p data [5] near the $p\bar{p}$ threshold [3]. We note that these two novel states are not predicted $q\bar{q}$ meson states in quark models and their closeness to the $N\bar{N}$ threshold suggests molecular structure (if they indeed exist), although hybrid or exotic structure can not be ruled out without direct observation and a detailed study of decay modes. All vector meson resonance (ground and excited state) coupling constants, $C_V(M)$, were fit to the available π^+,K^+,K^0 form factor data respecting the universality constraints and using our parametrized propagator solutions with Eq. (53). The experimental data is taken from several sources listed in Ref. [29] (we do not distinguish data points from different experiments). Older references can be found in the review by Gourdin [30]. The ground state ρ,ω,ϕ couplings are fairly well known from independent measurements, however, we allow for small variations in the couplings to optimize our fits while restricting the relative magnitude of the isoscalar couplings $C_\omega(K)=\frac{1}{2}C_\phi(K)$ to be consistent with the three-pole (naive) VMD prediction for the K^+ and K^0 form factors (known to be a very good approximation). This constraint on the ω and ϕ couplings also

TABLE I. Vector meson parameters. Underlined masses and widths correspond to the ρ''' and ω''' resonance parameters determined in Ref. [3]. All other resonances have mass and width values quoted in Ref. [28]. The δ_V entries are calculated from Eq. (17) with $M_V\Gamma_V(s)$ described in text.

V	M_V [GeV]	Γ_V [GeV]	C_V	δ_V	β_V	ξ_V	γ_V
ρ	0.768	0.151	1.02	0.145	1.040	−0.10	1.42
ρ'	1.465	0.310	0.02	0.118	0.966	0.05	1.30
ρ''	1.700	0.235	−0.02	0.075	0.954	0.05	1.30
ρ'''	2.150	0.220	−0.02	0.053	0.901	0.05	1.40
ω	0.782	0.008	0.175	0.008	1.027	−0.10	1.40
ω'	1.419	0.174	0.010	0.069	0.906	0.05	1.40
ω''	1.649	0.220	−0.045	0.073	0.965	0.05	1.30
ω'''	1.830	0.010	0.003	0.003	0.971	0.05	1.30
ϕ	1.019	0.004	0.35	0.002	0.986	0.0	1.40

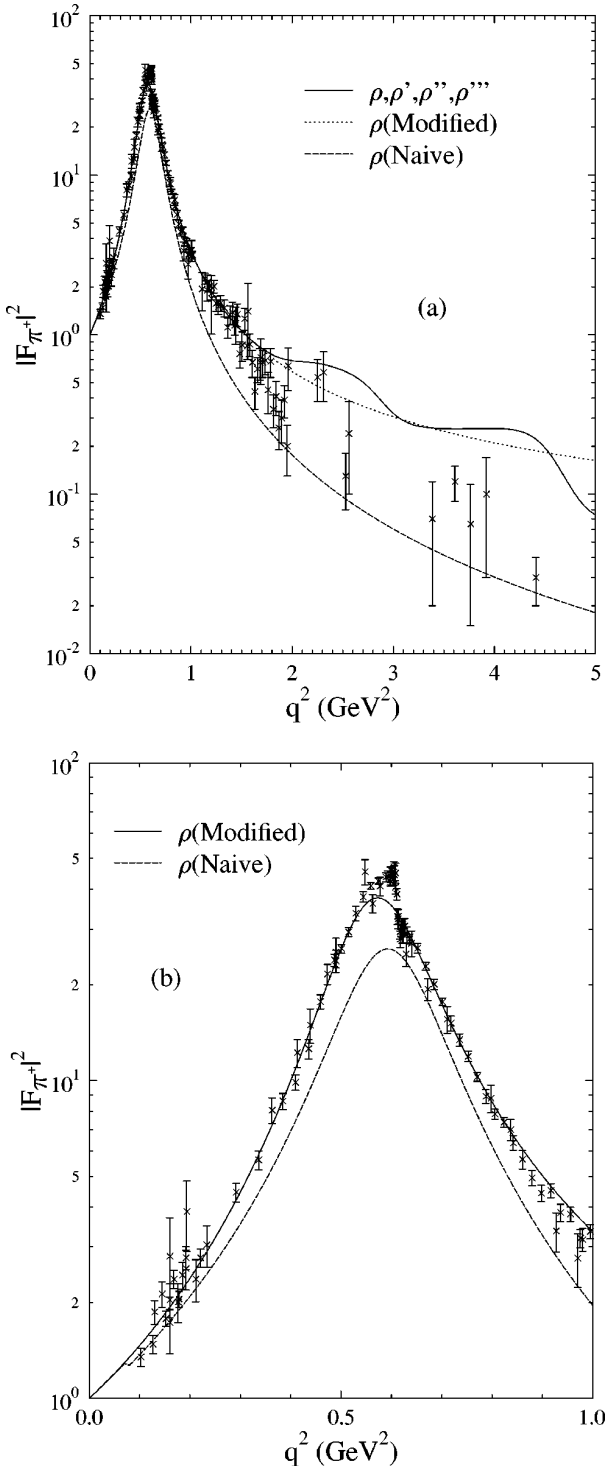

FIG. 4. (a) Square of the π^+ form factor in the timelike region comparing results of naive ρ dominance (dashed line), modified ρ dominance (dotted line), and the full calculation including propagator corrections and excited isovector resonances (solid line). (b) Blow-up of the squared π^+ form factor near the $\rho(770)$ resonance comparing naive ρ dominance (dashed line) and modified ρ dominance with propagator corrections (solid line).

corresponds to taking ideal mixing, $\tan\theta = 1/\sqrt{2}$, in Eqs. (5),(6) with $f_\omega^{-1}/f_\phi^{-1} = 1/\sqrt{2}$. All vector meson parameters are listed in Table I.

In Fig. 4(a) we present our model pion form factor in the timelike region with all excited states and propagator corrections (solid line) (from now on denoted full) and ρ dominance with modified propagator (dotted line) compared with the naive ρ-dominance prediction (dashed line). Near the ρ peak [where $\Sigma_\rho(M_\rho^2) = 0$], magnified in Fig. 4(b), the observed enhancement is due to the finite width correction factor δ_ρ. The data also shows a signature of the well-known ρ-ω mixing effect (i.e., small ω peak) which we have neglected. For $q^2 > M_\rho^2$ the modified ρ-dominance curve of Fig. 4(a) shows additional enhancement (i.e., not simply a constant times the naive VMD curve). Note in Fig. 3 that $\Sigma_\rho(s)$ is positive definite (vanishing at M_ρ^2) and thus produces propagator suppression for spacelike momentum transfer ($q^2 < 0$) and enhancement for timelike $q^2 > M_\rho^2$. Additional timelike enhancement comes from the energy-dependent γ-V coupling. The modified ρ-dominance curve reduces to the naive ρ-dominance curve as $\delta_\rho \to 0$. We do not treat δ_ρ as a free parameter (which would be slightly reduced in an optimal fit) since its value is constrained by our model LHC form factor and Eq. (17). The available pion data for $q^2 > 2.0$ GeV^2 is insufficient (with few points and low precision) to unambiguously assess the contributions of excited states. We note that our full calculation showing excited state oscillations has a suggestive shape compatible with the pion data except for the modified ρ-tail contribution being too large.

In Fig. 5(a) we plot the spacelike pion form factor with the same curve labeling as Fig. 4(a). The modified ρ-dominance result shows significant improvement with respect to the data points near $q^2 = -2$ GeV^2 and $q^2 = -3.4$ GeV^2 compared with the naive ρ-dominance result. The excited state contributions produce a small effect in the spacelike region (as expected). Extrapolating our model result to higher spacelike $|q^2|$, we note that our modified VMD pion form factor has a node at $q^2 \approx -6$ GeV^2. The position of this node is very sensitive to the finite width enhancement factor δ_ρ, as demonstrated in Fig. 5(b). The node disappears when $\delta_\rho \to 0$ (i.e., naive VMD does not produce a node). Similarly, if the naive VMD form Eq. (10) is used together with the modified ρ propagator, the resulting pion form factor also does not have a node. It follows that the node structure is a consequence of the once subtracted dispersion relation together with the energy-dependent γ-V interaction assumed for the spectral density and a questionable propagator extrapolation. We caution that the asymptotic behavior of our propagator modifications are not well constrained and other dynamics such as nonleading LHC and/or perturbative QCD effects become increasingly important for large spacelike q^2, and thus a naive extrapolation of our model is unjustified. We are therefore suspicious of placing predictive significance to the observed nodal signature of our model, but only point it out as a curious conspiracy of model-dependent effects.

In Fig. 6(a) we plot the squared kaon form factor in the timelike region comparing our full result with naive and modified ρ, ω, ϕ dominance. The contribution from the modified ρ spectral function produces most of the difference between the naive and modified ρ, ω, ϕ dominance curves since the ϕ and ω propagator corrections and coupling constant differences are very small. Note that our full result does not reproduce the nearly constant q^2 dependence seen in the precise data between $1.4 \leq q^2 \leq 2.0$ GeV^2. Since there is no broad resonance in this region, we speculate that this shoul-

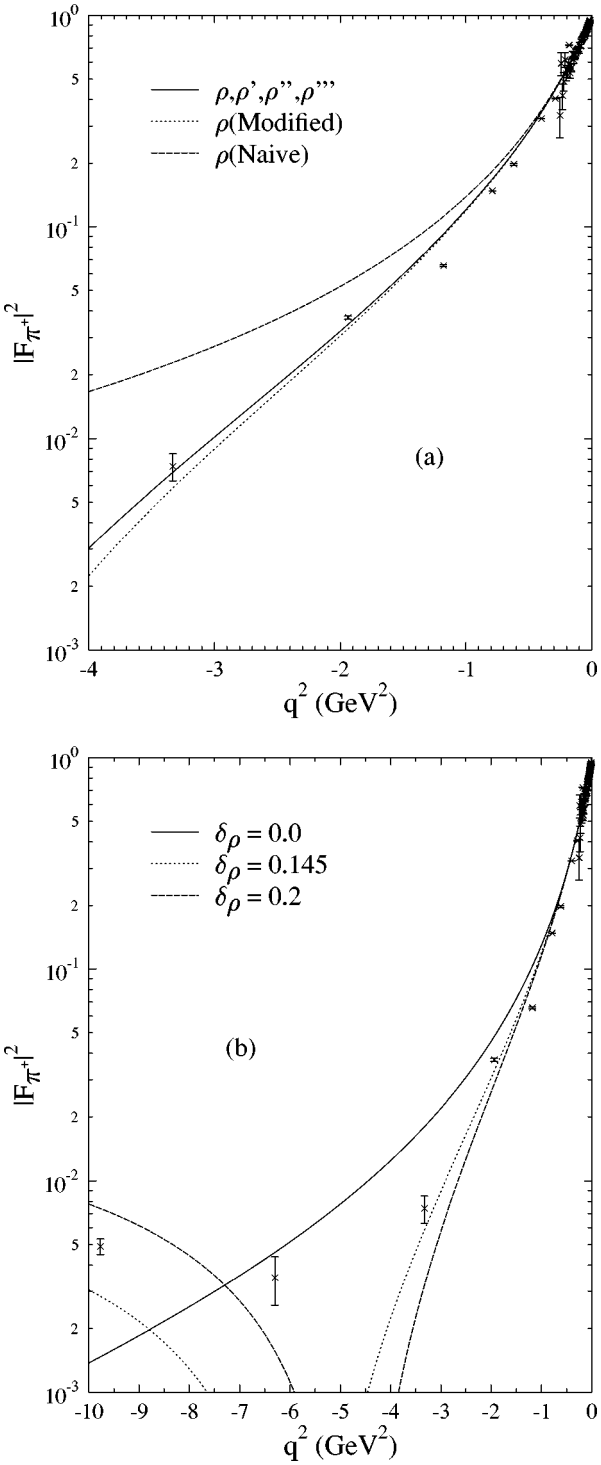

FIG. 5. (a) Square of the π^+ form factor in the spacelike region comparing results of naive ρ dominance (dashed line), modified ρ dominance (dotted line), and the full calculation including propagator corrections and excited isovector resonances (solid line). (b) Square of the π^+ form factor in the spacelike region at larger $|q^2|$ showing nodal structure of modified ρ dominance and sensitivity to δ_ρ.

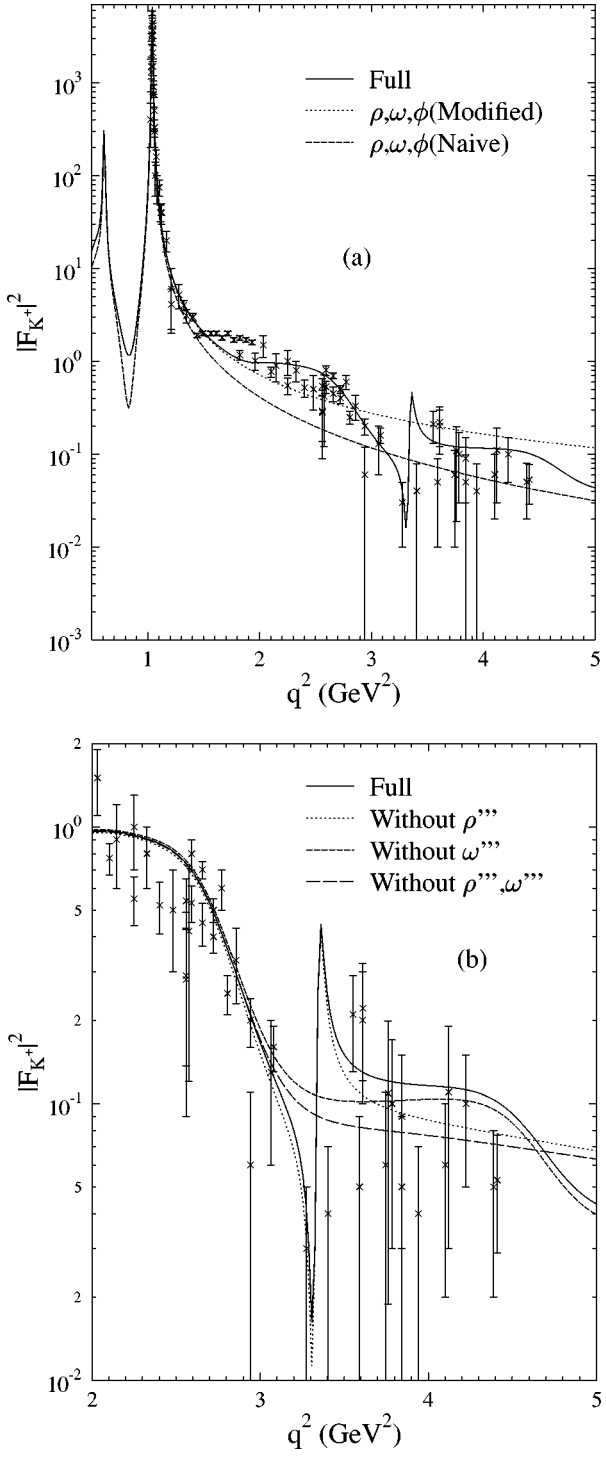

FIG. 6. (a) Square of the K^+ form factor in the timelike region comparing the results of naive VMD (dashed line), modified VMD (dotted line), and the full calculation including propagator corrections and excited resonances (solid line). (b) Blow-up of the squared K^+ form factor near the unconfirmed $\omega'''(1830)$ and $\rho'''(2150)$ resonance region comparing results including all excited states (solid line), without the ρ''' (dotted line), without the ω''' (short dashed line), and without both ρ''' and ω''' (long dashed line). All curves are calculated using modified propagators.

der feature may be the consequence of strong coupling to the inelastic channel $\phi\pi \to K\overline{K}$ with a threshold near $q^2 = 1.35$ GeV^2. We present a blow-up of the timelike ρ''' and ω''' region in Fig. 6(b) showing the results including different combinations of these unconfirmed states. The data is not precise enough to strongly distinguish between the different possibilities, however, the data cannot rule out the possible existence of a narrow resonance structure near $q^2 \sim 3.4$ GeV^2.

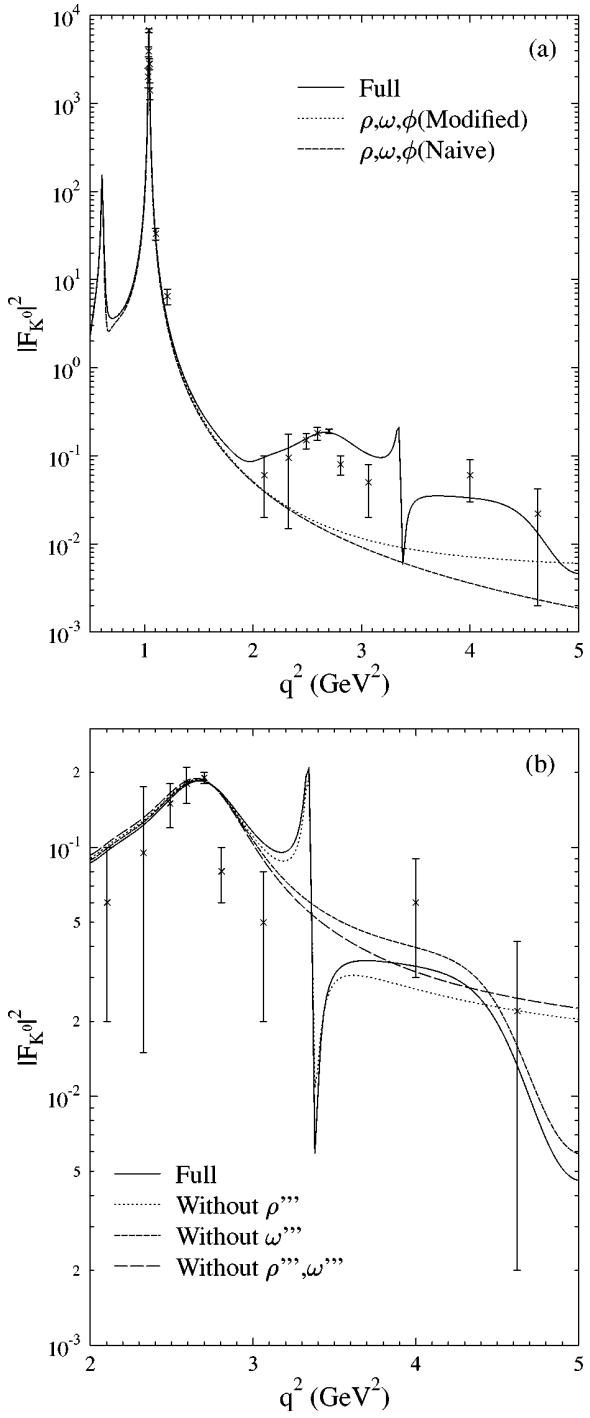

FIG. 7. (a) Square of the K^0 form factor in the timelike region comparing the results of naive VMD (dashed line), modified VMD (dotted line), and the full calculation including propagator corrections and excited resonances (solid line). (b) Blow-up of the squared K^0 form factor near the unconfirmed $\omega'''(1830)$ and $\rho'''(2150)$ resonance region comparing results including all excited states (solid line), without the ρ''' (dotted line), without the ω''' (short-dashed line), and without both ρ''' and ω''' (long dashed line). All curves are calculated using modified propagators.

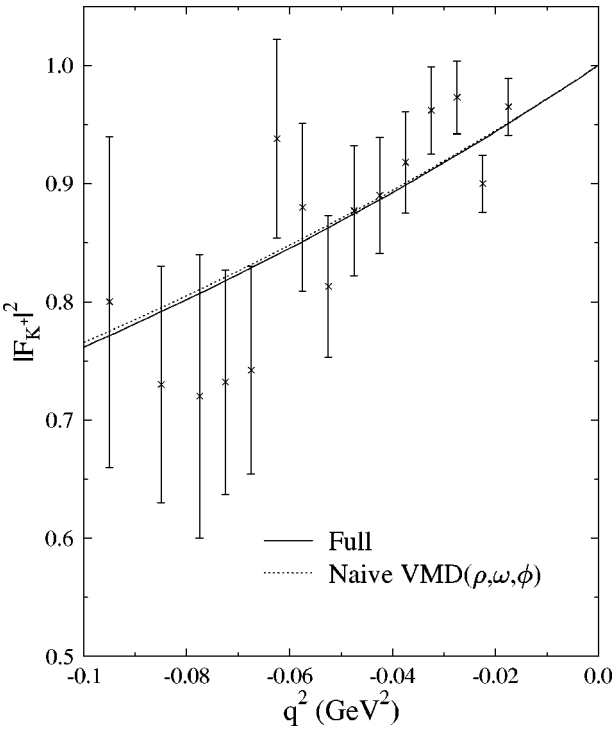

FIG. 8. Square of the K^+ form factor in the spacelike region comparing the results of naive VMD (dotted line), and the full calculation including propagator corrections and excited resonances (solid line).

In Fig. 7(a) we present the squared K^0 timelike form factor comparing the full, naive and modified ρ,ω,ϕ dominance results. The contributions from excited states provide a significant improvement with respect to the data compared with the naive and modified ρ,ω,ϕ dominance results. In Fig. 7(b), we present the timelike K^0 results corresponding to different combinations of the unconfirmed resonances. Again, the present data does not have sufficient precision to discriminate between the different possibilities.

We present our results for the spacelike K^+ and K^0 form factors in Figs. 8 and 9, respectively. Our full calculation is nearly degenerate with the naive ρ,ω,ϕ dominance result of the spacelike K^+ form factor for small $|q^2|$. The modifications to naive VMD produce substantial enhancement in the spacelike K^0 form factor as seen in Fig. 9. When all of the finite width δ_V correction factors are artificially set to zero, all of the propagator modifications vanish and we recover the naive VMD result with a small deviation due to excited state contributions and coupling constant differences. The full K^0 form factor result (solid line) becomes nearly constant at large spacelike q^2, which conflicts the expectation of pQCD scaling. This result shows that a once subtracted dispersion relation can produce unphysical behavior when analytic continuation is extended far away from the subtraction point if the spectral function does not have the correct asymptotic behavior or does not satisfy additional sum rule constraints. Specifically, if we demand the K^0 form factor to vanish at $s=\pm\infty$, we can take the limit of the dispersion relation Eq. (14) to obtain a superconvergence constraint

$$\lim_{s\to\pm\infty}\mathrm{Re}[F_{K^0}(s)]=\mp\frac{1}{\pi}\int_{s_0}^{\infty}\frac{ds'}{s'}\mathrm{Im}[F_{K^0}(s')]\to 0. \quad (54)$$

Obviously, the asymptotic power behavior of the spectral function must be restricted $\mathrm{Im}[F_{K^0}(s)]\propto s^p$, where $p<0$, otherwise the integral will diverge. Our model spectral func-

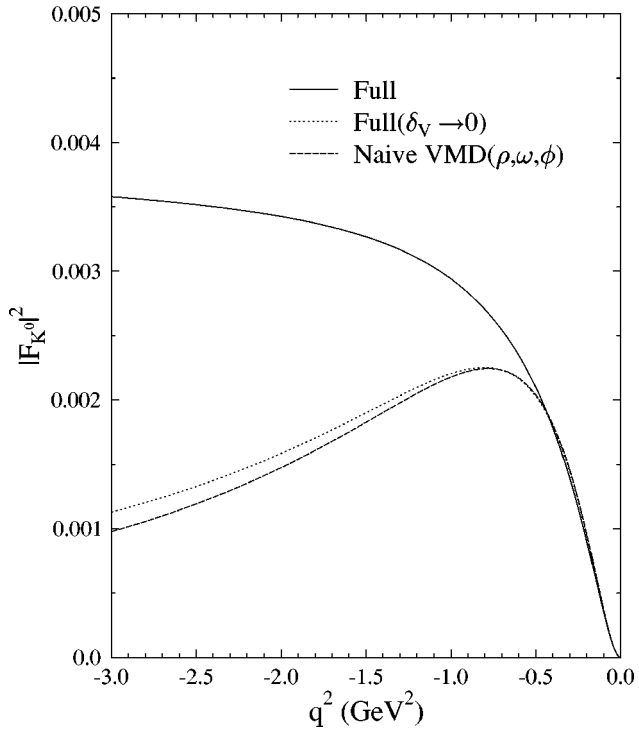

FIG. 9. Square of the K^0 form factor in the spacelike region comparing results including all excited states and propagator corrections (solid line), including all excited states and bare propagators (dotted line), and naive VMD (dashed line).

tions do converge term by term, yielding finite constants after integration, however, the superconvergence is violated because there is not a perfect cancellation of the total area (weighted by $1/s$). Although it is possible to enforce superconvergence relations to further constrain the vector meson parameters, this is probably unjustified since the asymptotic behavior of the propagator modifications are highly uncertain (model dependent) and other contributions such as inelastic threshold effects should be included, consistently constrained by multichannel unitarity.

VI. CONCLUSIONS

We have attempted to incorporate several modifications to naive VMD in order to study: observable effects from finite width propagator corrections, the physical consequences of using once subtracted dispersion relations with a gauge invariant γ-V interaction, and to test whether or not existing timelike data shows resonance structure compatible with the existence of two unconfirmed vector states near the $p\bar{p}$ threshold. We derived resonant propagator modifications by incorporating nonresonant LHC vector meson exchange amplitudes in the single channel N/D approximation with elastic unitarity. We find the ρ propagator modifications and coupling constant renormalization are crucial for a quantitative VMD type description of the enhancement observed in the timelike pion data near and above the ρ peak. Our calculated ρ enhancement factor $\delta_\rho = 0.145$ is consistent with the observed timelike enhancement near the ρ peak $\delta_\rho^{\rm exp} = 0.13 \pm 0.08$. We also investigated the reliability of Sakurai's $SU_F(3)$ universality symmetry for vector meson couplings since the timelike data exposes and constrains the resonance contributions. By comparing the relative strength of resonance couplings between the pion and kaon, we have verified that $SU_F(3)$ universality symmetry is a good approximation for the couplings of both the low-lying and excited vector meson states to the light psuedoscalar mesons. We observe interesting nodal structure at large spacelike q^2 in the pion form factor resulting from a conspiracy of effects due to our use of once subtracted dispersion relations with energy-dependent γ-V interactions and (questionable) extrapolated asymptotic behavior of the propagator modifications. The present meson form factor data does not have sufficient precision to make definitive conclusions about the existence and/or properties (i.e., mass, widths, or couplings) of the unconfirmed $\rho'''(2150)$ and $\omega'''(1830)$ resonance states, however, the present data does not exclude the possibility of their existence. We suggest that new e^+e^- experiments looking for novel vector states (e.g., molecules, hybrids, exotics) beyond the standard $q\bar{q}$ quark model expectations should explore energies near $\sqrt{s} = 1.83, 2.15$ GeV in multimeson channels to confirm and establish the structure of resonance states indicated by the LEAR data.

ACKNOWLEDGMENT

This work was supported by NSF Grant No. HRD-9633750.

APPENDIX: N/D METHOD

We present here a review of the single channel N/D method. Further details can be found in [1,2]. The method is derived from the assumption that partial wave scattering amplitudes $A_l(s)$ are analytic functions possessing singularities and cut discontinuites governed by unitarity. For equal mass (e.g., $\pi\pi$) two-body elastic scattering, unitarity dictates that the amplitude must possess a right hand cut (RHC) discontinuity for $s_R \leqslant s \leqslant \infty$ and a left hand cut (LHC) discontinuity for $-\infty \leqslant s \leqslant s_L$, where $s_R = 4M_\pi^2$ and $s_L = 4M_\pi^2 - M_\rho^2$, assuming the ρ meson is the lightest exchanged particle in the t and u channel. Applying Cauchy's theorem to a countour distorted around the LHC and RHC,

$$A_l(s) = \frac{1}{2\pi i} \oint_C \frac{ds'}{s'-s} A_l(s'), \tag{A1}$$

$$= \frac{1}{\pi} \int_{-\infty}^{s_L} \frac{ds'}{s'-s} \mathrm{Im}[A_l(s')] + \frac{1}{\pi} \int_{s_R}^{\infty} \frac{ds'}{s'-s} \mathrm{Im}[A_l(s')], \tag{A2}$$

the analytic amplitude receives only LHC and RHC contributions (assuming proper convergence at $|s| \to \infty$). The imaginary part of $A_l(s)$ is governed by unitarity for $s \geqslant s_R$

$$\mathrm{Im}[A_l(s)] = \sqrt{\frac{s-s_R}{s}} |A_l(s)|^2, \tag{A3}$$

adopting a convenient amplitude normalization. Cauchy's theorem then reduces to a nonlinear integral equation

$$A_l(s)=\frac{1}{\pi}\int_{-\infty}^{s_L}\frac{ds'}{s'-s}\mathrm{Im}[A_l(s)] + \frac{1}{\pi}\int_{s_R}^{\infty}\frac{ds'}{s'-s}\sqrt{\frac{s-s_R}{s}}|A_l(s)|^2. \quad \text{(A4)}$$

The N/D method provides a self-consistent solution to this equation. The essential simplifications follow from representing the solution as a ratio (writing the threshold energy dependence explicitly)

$$A_l(s)=(s-s_R)^l\frac{N_l(s)}{D_l(s)}, \quad \text{(A5)}$$

where $N_l(s)$ has only LHC and $D_l(s)$ has only RHC discontinuities, respectively, and realizing the elastic unitarity relation for the inverse imaginary amplitude is purely kinematic

$$\mathrm{Im}[A_l^{-1}(s)]=\frac{\mathrm{Im}[A_l^*(s)]}{|A_l(s)|^2}=-\sqrt{\frac{s-s_R}{s}}. \quad \text{(A6)}$$

Defining the LHC discontinuity function $f_l(s)$,

$$f_l(s)\equiv\mathrm{Im}[A_l(s)] \quad (s<s_L), \quad \text{(A7)}$$

coupled linear integral equations are obtained for $N_l(s)$ and $D_l(s)$,

$$N_l(s)=\frac{1}{\pi}\int_{-\infty}^{s_L}\frac{f_l(s')}{(s'-s)(s'-s_R)^l}D_l(s')ds', \quad \text{(A8)}$$

$$D_l(s)=\delta_l-\frac{(s-s_0)}{\pi}\int_{s_R}^{\infty}\frac{(s'-s_R)^{l+1/2}}{\sqrt{s'}(s'-s)(s'-s_0)}N_l(s')ds', \quad \text{(A9)}$$

where

$$\mathrm{Im}[N_l(s)]=\frac{f_l(s)D_l(s)}{(s-s_R)^l} \quad (s<s_L), \quad \text{(A10)}$$

$$\mathrm{Im}[D_l(s)]=-\sqrt{\frac{s-s_R}{s}}(s-s_R)^lN_l(s) \quad (s>s_R). \quad \text{(A11)}$$

We have assumed a single subtraction for $D_l(s)$ at the arbitrary point s_0, $\delta_l=D_l(s_0)$. Note the real (principal value) part of Eq. (A9) with $l=1$ and $s_0=0$ corresponds to the modified resonance propagator disperion relation Eq. (16). Back substituting Eq. (A8) into Eq. (A9) (and vice versa), the dispersion relations are decoupled yielding Freedholm-type integral equations

$$D_l(s)=\delta_l+\int_{-\infty}^{s_L}K_l(s,s'')f_l(s'')D_l(s'')ds'', \quad \text{(A12)}$$

depending on the LHC discontinuity function $f_l(s)$, and with the kernel defined

$$K_l(s,s'')=\frac{(s-s_0)}{\pi^2(s''-s_R)^l}\int_{s_R}^{\infty}\sqrt{\frac{s'-s_R}{s'}}\times\frac{(s'-s_R)^lds'}{(s'-s)(s'-s_0)(s'-s'')}. \quad \text{(A13)}$$

Similarly, the $N_l(s)$ function satisfies

$$N_l(s)=\frac{1}{\pi}\int_{-\infty}^{s_L}\frac{f_l(s')}{(s'-s)(s'-s_R)^l}\left[\delta_l-\frac{(s'-s_0)}{\pi}\times\int_{s_R}^{\infty}\frac{(s''-s_R)^{l+1/2}N_l(s'')}{\sqrt{s''}(s''-s')(s''-s_0)}ds''\right]ds', \quad \text{(A14)}$$

$$=\delta_lB_l(s)+\frac{1}{\pi}\int_{s_R}^{\infty}\frac{[(s'-s_0)B_l(s')-(s-s_0)B_l(s)]}{(s'-s)(s'-s_0)}\times\sqrt{\frac{s'-s_R}{s'}}(s'-s_R)^lN_l(s')ds', \quad \text{(A15)}$$

where $B_l(s)$ is the nonresonant partial wave Born amplitude

$$B_l(s)=\frac{1}{\pi}\int_{-\infty}^{s_L}\frac{f_l(s')ds'}{(s'-s)(s'-s_R)^l}, \quad \text{(A16)}$$

calculated in terms of the LHC discontinuity function $f_l(s)$. In this work we truncate the self-consistent Eq. (A15), taking the LHC N function in the Born approximation, although we employ a $\rho\pi\pi$ vertex function which models the self-consistent $N(D)$ functional dependence. Also, we have taken advantage of the Castillejo, Dalitz, and Dyson (CDD) ambiguity [31] to ensure vector meson propagator poles independent of the strength and functional behavior of the LHC amplitudes. The CDD ambiguity addresses the fact that the N/D solution for $A_l(s)$ is not unique. It is possible to add arbitrary poles to $D_l(s)$ without spoiling $A_l(s)$ as a solution of the dispersion relation Eq. (A4). The CDD poles have the physical interpretation of *elementary particles*, in the sense that these poles persist even for arbitrarily weak LHC interactions. Without CDD poles, solutions of the N/D equations producing zeros in the D function are *dynamical* boundstates or resonances which only develop if the LHC produces attraction with strength exceeding some critical value. Recalling our definition of the modified propagators, Eq. (15), we require all of the vector mesons to possess CDD poles since we have made the replacement

$$D^{l=1}_{\pi\pi;V}(s)\to\Delta_V^{l=1}(s)=(M_V^2-s)+D^{l=1}_{\pi\pi;V}(s), \quad \text{(A17)}$$

which reduces to the bare (elementary) vector meson propagator in the limit of vanishing LHC amplitudes.

[1] Hugh Burkhardt, *Dispersion Relation Dynamics* (North-Holland, Amsterdam, 1969).
[2] S. C. Frautschi, *Regge Poles and S-Matrix Theory* (Benjamin, New York, 1963).
[3] R. A. Williams, S. Krewald, and K. Linen, Phys. Rev. C **43**, 452 (1995).
[4] R. A. Williams and C. P. Truman, Phys. Rev. C **53**, 1580 (1996).
[5] G. Bardin *et al.*, Phys. Lett. B **255**, 149 (1991); **257**, 514 (1991).
[6] E. Luppi, Nucl. Phys. **A558**, 165c (1993).
[7] J. J. Sakurai, Ann. Phys. (N.Y.) **11**, 1 (1960).
[8] J. J. DeSwart, Rev. Mod. Phys. **35**, 916 (1963).
[9] S. Okubo, Phys. Lett. **5**, 165 (1963); G. Zweig, CERN Report No. 8419/TH412, 1964; I. Iizuka, Prog. Theor. Phys. **38**, 21 (1966).
[10] R. A. Williams, Phys. Rev. C **57**, 223 (1998).
[11] M. Benayoun, S. Eidelman, K. Maltman, H. B. O'Connell, B. Shwartz, and A. G. Williams, Proceedings of APCTP Workshop: Pacific Particle Physics Phenomenology, P4, 1997, hep-ph/9707509.
[12] K. Nishijima, Phys. Rev. **122**, 298 (1961).
[13] J. C. Ward, Phys. Rev. **78**, 1824 (1950).
[14] Y. Takahashi, Nuovo Cimento **6**, 370 (1957).
[15] T. E. Rudy, H. W. Fearing, and S. Scherer, Phys. Rev. C **50**, 447 (1994); **50**, 447 (1994).
[16] G. J. Gounaris and J. J. Sakurai, Phys. Rev. Lett. **21**, 244 (1968); G. J. Gounaris, Phys. Rev. **181**, 2066 (1969).
[17] F. M. Renard, Phys. Lett. **47B**, 361 (1973).
[18] G. F. Chew and S. Mandelstam, Phys. Rev. **119**, 467 (1960).
[19] F. Zachariasen, Phys. Rev. Lett. **7**, 112 (1961).
[20] F. Zachariasen and C. Zemach, Phys. Rev. **128**, 849 (1962).
[21] B. H. Bransden, I. R. Gatland, and J. W. Moffat, Phys. Rev. **128**, 859 (1962).
[22] L. A. P. Balazs, Phys. Rev. **134**, B1315 (1964).
[23] M. L. Mehta, Phys. Rev. **134**, B1377 (1964).
[24] R. C. Arnold, Phys. Rev. **134**, B1380 (1964).
[25] F. Zachariasen, in *Strong Interactions and High Energy Physics*, edited by R. G. Moorhouse (Oliver and Boyd, London, 1964).
[26] J. E. Augustin *et al.*, Nuovo Cimento **2**, 214 (1969).
[27] D. Benaksas *et al.*, Phys. Lett. **39B**, 289 (1972).
[28] Particle Data Group, L. Montanet *et al.*, Phys. Rev. D **50**, 1443 (1994).
[29] S. R. Amendolia *et al.*, Nucl. Phys. **B277**, 168 (1986); L. M. Barkov *et al.*, *ibid.* **B256**, 365 (1985); P. M. Ivanov *et al.*, Phys. Lett. **107B**, 297 (1981); B. Delcourt *et al.*, *ibid.* **99B**, 257 (1981); F. Mane *et al.*, *ibid.* **99B**, 261 (1981); B. Esposito *et al.*, Lett. Nuovo Cimento **28**, 337 (1980); C. J. Bebek *et al.*, Phys. Rev. D **17**, 1693 (1978); A. Quenzer *et al.*, Phys. Lett. **76B**, 512 (1978); A. D. Bukin *et al.*, *ibid.* **73B**, 226 (1978); B. Esposito *et al.*, *ibid.* **67B**, 239 (1977); F. Vannucci *et al.*, Phys. Rev. D **15**, 1814 (1977); G. Cosme *et al.*, Phys. Lett. **63B**, 349 (1976); D. Bollini *et al.*, Lett. Nuovo Cimento **14**, 418 (1975); M. Bernardini *et al.*, Phys. Lett. **46B**, 261 (1973); V. E. Balakin *et al.*, *ibid.* **34B**, 328 (1971); J. E. Augustin *et al.*, *ibid.* **28B**, 508 (1969).
[30] M. Gourdin, Phys. Rep., Phys. Lett. **11C**, 29 (1974).
[31] L. Castillejo, R. H. Dalitz, and F. J. Dyson, Phys. Rev. **101**, 453 (1956).